# Unitary synaptic currents between lacunosum-moleculare interneurones and pyramidal cells in rat hippocampus

Sandrine Bertrand and Jean-Claude Lacaille

*Centre de recherche en sciences neurologiques, Département de physiologie, Université de Montréal, CP 6128, succ. Centre Ville, Montréal, Québec, Canada H3C 3J7*

(Received 31 August 2000; accepted after revision 6 December 2000)

1. Unitary inhibitory postsynaptic currents (uIPSCs) were characterised between 23 synaptically coupled interneurones at the border of stratum radiatum and lacunosum-moleculare (LM) and CA1 pyramidal cells (PYR) using dual whole-cell recordings and morphological identification in rat hippocampal slices.

2. LM interneurones presented a morphology typical of stellate cells, with a fusiform soma as well as dendritic and axonal arborisations in stratum radiatum and lacunosum-moleculare.

3. Single spikes in interneurones triggered uIPSCs in pyramidal cells that were blocked by the $GABA_A$ antagonist bicuculline and mediated by a chloride conductance. The latency, rise time, duration and decay time constant of uIPSCs were a function of amplitude in all pairs, suggesting a homogeneity in the population sampled.

4. During paired pulse stimulation, individual LM–PYR connections exhibited facilitation or depression. The paired pulse ratio was inversely related to the amplitude of the first response. The transition from facilitation to depression occurred at 26 % of the maximal amplitude of the first uIPSC. Paired pulse depression was not modified by CGP 55845 and thus was $GABA_B$ receptor independent.

5. CGP 55845 failed to modify the amplitude of uIPSCs, suggesting an absence of tonic presynaptic $GABA_B$ inhibition at LM–PYR connections.

6. Increasing GABA release by repetitive activation of interneurones failed to induce $GABA_B$ IPSCs. With extracellular minimal stimulation, increasing stimulation intensity above threshold, or repetitive activation, evoked $GABA_B$ IPSCs, probably as a result of coactivation of several GABAergic fibres.

7. Thus, dendritic inhibition by LM interneurones involves $GABA_A$ uIPSCs with kinetics dependent on response amplitude and subject to $GABA_B$-independent paired pulse plasticity.

The knowledge of intrinsic membrane properties of single cells within a neuronal network is necessary but insufficient to comprehend the physiology of an assembly of neurones. An understanding of how these cells communicate with each other to produce a well-adapted pattern of activity is also essential. The hippocampal formation is a complex cortical network which is important for memory processes (Collingridge, 1987), but which is also implicated in pathological conditions like epilepsy (Prince, 1978). This neuronal network consists of glutamatergic projection pathways, i.e. granule cells of the dentate gyrus and pyramidal cells of CA3 and CA1, and of a variety of interneurones shown to be nearly all GABAergic (Woodson *et al.* 1989). These interneurones produce a powerful inhibition of excitatory cells and appear highly important in the regulation of their activity (for review see Freund & Buzsaki, 1996). Indeed, rhythmic inhibition of pyramidal cells by hippocampal interneurones may generate oscillatory activity important for the integration of synaptic inputs and memory formation (Buzsaki & Chrobak, 1995; Perez *et al.* 1999; Chapman & Lacaille, 1999). Based on their morphology, membrane properties and connectivity, hippocampal GABAergic interneurones can be divided into distinct populations (see Buhl *et al.* 1994*a*; Freund & Buzsaki, 1996). Although these interneurones have been extensively studied, little information is available on the properties of unitary synaptic currents produced by identified individual interneurones on pyramidal cells (Jiang *et al.* 2000; Maccaferri *et al.* 2000).

In the hippocampus, the actions of GABA are mediated by two receptor types. Activation of $GABA_A$ receptors triggers a fast hyperpolarisation due to an increase in $Cl^-$

conductance (Alger & Nicoll, 1982). In contrast, slower effects are produced by activating $GABA_B$ receptors that are coupled to G-proteins. Depending on the $GABA_B$ receptor localisation, two distinct responses can be observed. At the postsynaptic level, activation of $GABA_B$ receptors leads to an increase in $K^+$ currents (Dutar & Nicoll, 1988), while at the presynaptic level, it blocks $Ca^{2+}$ currents (Dolphin, 1995). Some evidence suggests that distinct GABAergic interneurones could be specialised for certain types of inhibition, i.e. $GABA_A$ and (or) $GABA_B$ (for review see Nurse & Lacaille, 1997). However, most studies with stimulation of individual interneurones and recording unitary GABA responses have uncovered only $GABA_A$ synaptic mechanisms (Jiang *et al.* 2000; Maccaferri *et al.* 2000; Scanziani, 2000; but see Thomson & Destexhe, 1999). In addition, the kinetics and plasticity of $GABA_A$ unitary inhibitory postsynaptic currents (uIPSCs) generated in the pyramidal cells by different interneurone subtypes, appear heterogeneous (Pearce *et al.* 1995; Ouardouz & Lacaille, 1997; Jiang *et al.* 2000; Maccaferri *et al.* 2000). This heterogeneity applies to interneurones across and within specific layers (Jiang *et al.* 2000; Maccaferri *et al.* 2000). Given the importance of GABAergic inhibition in normal and pathological hippocampal function, it seems crucial to understand better the properties of individual synapses made by different types of GABAergic interneurones.

Stellate cells are interneurones located near the border of stratum radiatum and stratum lacunosum-moleculare (LM) which provide feedforward dendritic inhibition of CA1 pyramidal cells (Lacaille & Schwartzkroin, 1988; Vida *et al.* 1998). In addition, these interneurones generate intrinsic theta-frequency oscillations which can lead to rhythmic inhibition and pacing of firing of pyramidal cells (Chapman & Lacaille, 1999). However, the mechanisms at stellate cell–pyramidal neurone synapses remain unclear. Stimulation with glutamate of unidentified interneurones in LM was found to activate $GABA_B$-mediated IPSPs in pyramidal cells (Williams & Lacaille, 1992), but stimulation of individual interneurones in LM produced only $GABA_A$ unitary responses in pyramidal cells (Ouardouz & Lacaille, 1997; Vida *et al.* 1998). To characterise the properties of dendritic synapses made by LM interneurones on CA1 pyramidal cells (Lacaille & Schwartzkroin, 1988), paired whole-cell recordings were obtained from interneurones in LM and CA1 pyramidal cells in rat hippocampal slices in combination with intracellular labelling to morphologically identify pre- and postsynaptic cell types. More specifically, we determined the properties of unitary IPSCs between these cells and their paired pulse modulation.

## METHODS

### Slice preparation and recordings

All experiments were carried out according to the guidelines laid down by our local Animal Care Committee at the University of Montréal. Male Sprague Dawley rats (21–35 days old) were deeply anaesthetised with halothane prior to decapitation. The brain was quickly removed and placed in cold artificial cerebrospinal fluid (ACSF) containing (mM): NaCl 124; KCl 2.5; $NaH_2PO_4$ 1.25; $NaHCO_3$ 26; $MgSO_4$ 2; $CaCl_2$ 2; glucose 10; saturated with 95% $O_2$ and 5% $CO_2$ (pH= 7.4). Transverse hippocampal slices (300 $\mu$m) were cut with the aid of a vibroslicer and transferred to a holding chamber for at least 1 h prior to recordings. For whole-cell recordings, a slice was submerged in a chamber mounted on an upright microscope (Zeiss Axioskop FS, Jena, Germany) equipped with Hoffman optics (Modulation Optics, Greenvale, NY, USA), a ×40 immersion objective lens and an infrared video camera (Cohu 6500, San Diego, CA, USA). Throughout the experiments, a high $Ca^{2+}$–high $Mg^{2+}$ solution (containing (mM): NaCl 124; KCl 2.5; $NaH_2PO_4$ 1.25; $NaHCO_3$ 26; $MgSO_4$ 4; $CaCl_2$ 4; glucose 10) was superfused at a flow rate of 2.5–3 ml $min^{-1}$, to reduce spontaneous synaptic activity and allow accurate measurement of uIPSC time course. All solutions were applied at room temperature (22–24 °C). Whole-cell patch-clamp recordings were obtained using glass microelectrodes (3–7 MΩ) filled with a solution containing (mM): potassium gluconate 140; NaCl 5; EGTA 0.5; $MgCl_2$ 2; Hepes 0.5; phosphocreatine 10; ATP-Tris 2; GTP-Tris 0.4; pH adjusted to 7.2–7.4 with KOH. For a *post hoc* morphological analysis of the recorded cells, fluorescent dyes (0.05% fluorescein or Oregon Green in interneurones and tetramethylrhodamine in pyramidal cells; Molecular Probes, Eugene, OR, USA) or biocytin (0.1%) were added to the intracellular solution. Pyramidal cells were recorded in voltage-clamp mode using an Axopatch 200B amplifier, and interneurones in bridge mode using an Axoclamp 2A amplifier. Interneurones with a fusiform soma located near the border of stratum radiatum and stratum lacunosum-moleculare were selected (Williams *et al.* 1994; Fig. 1*A*1). After obtaining gigaohm seals (> 1 GΩ) on both cell types, each membrane was broken and the pair was tested for a synaptic connection by inducing multiple action potentials in the interneurone using a large current pulse injection. If the cells were synaptically coupled, unitary IPSCs were elicited using a single presynaptic action potential in the presence of glutamate receptor blockers. The mean series resistances of interneurones and pyramidal cells were measured and were, respectively, $34.5 \pm 2.8$ and $23.1 \pm 1.7$ MΩ ($n = 23$). Series resistance was not compensated during pyramidal cell voltage-clamp recordings. Data were digitised at 10 kHz and acquired on a PC. Glutamatergic non-NMDA and NMDA receptors were blocked with 6-cyano-7-nitroquinoxaline-2,3-dione (CNQX; 20 $\mu$M) and DL-2-amino-5-phosphopentanoic acid (AP5; 50 $\mu$M). CNQX and AP5 were purchased from RBI (Natick, MA, USA); bicuculline and 4-aminopyridine (4AP, 10 $\mu$M) from Sigma, and CGP 55845 was a gift from Novartis.

### Histology

After recordings, slices containing biocytin- or fluorescent dye-filled cells were fixed overnight with 4% paraformaldehyde in 0.1 M phosphate buffer. Slices were then washed and stored in 0.1 M phosphate buffer. To reveal biocytin, the slices were processed using the Vectastain ABC kit (Vector Laboratories, Burlingame, CA, USA) as previously described (Chapman & Lacaille, 1999). Slices were mounted with DPX mounting medium (Electron Microscopy Sciences, Ft Washington, PA, USA) and observed under a light microscope. Well-filled pairs of cells were traced with a camera lucida ($n = 2$). Slices with fluorescent dye-filled cells were cleared with methylsalicylate and mounted with antifading mounting medium: Fluoromount (VWR Canlab, Qc, Canada) or Prolong (Molecular Probes). These slices were then examined under a confocal microscope (BioRad, MRC 600). The fluorophores were excited using the 514 nm line of an argon ion laser. Fluorescein/Oregon Green were detected with a bandpass filter (525–555 nm), while tetramethylrhodamine was simultaneously detected using a long-pass filter (590 nm). The Z-series of the cells (steps 0.6–1.6 $\mu$m) were processed with Comos software (BioRad).

**Data analysis**

The analysis of uIPSCs (e.g. Fig. 1*B*1) was done using Axograph (Axon Instruments, Foster City, CA, USA). Each uIPSC was manually individualised into events of 100 ms with the interneurone spike as a reference (Fig. 1*B*2). The mean uIPSC was then calculated by averaging at least 20 uIPSCs. For each selected individual uIPSC, the analysis program determined the peak amplitude from the maximum peak value (peak) to the baseline (dashed line on Fig. 1*B*1). The latency of the uIPSC onset was defined as the time from the peak of the interneurone spike to 5% of the uIPSC peak amplitude, which was measured by averaging six points around the peak. Rise time was taken as the time taken for the current to rise from 20 to 80% of peak amplitude. The decay time constant was measured from monoexponential fits, starting from the region where IPSCs began to decay to the return to baseline (grey line on Fig. 1*B*1). In all cases, visual inspection indicated that the decay of uIPSCs was well fitted by a single exponential. The mean of each uIPSC parameter was obtained from at least 10 (range 10–669) individual uIPSC measurements in each cell, unless otherwise specified. Noise was defined as the standard deviation of the amplitude during a baseline interval of 50 ms recorded prior to the onset of the uIPSC. The uIPSC amplitude was significantly distinct from the noise in each connection studied. Failures were determined by visual inspection. Using this method, the amplitude of the smallest 10% of detected events was 24.8 ± 1.6 pA ($n = 5$ uIPSCs) in the LM–PYR pair with the largest noise level (11.7 ± 0.9 pA) and 6.8 ± 1 pA in the pair with the smallest noise (2.8 ± 0.2 pA, $n = 4$ events). In pairs with a noise level close to the mean value (7.34 ± 0.5 pA), the amplitude of the smallest 10% of detected events was 15.3 ± 1.9 pA ($n = 5$ pairs). The possibility of sampling spontaneous events in high-failure-rate pairs was reduced by applying numerous presynaptic stimulations (up to 1000) and by visually distinguishing uIPSCs by their shape and latency. Statistical analysis was performed on raw data. The data were checked for normal distribution. Student's $t$ tests were performed to compare two series of paired data. A two-way ANOVA was carried out in order to test the significance in several

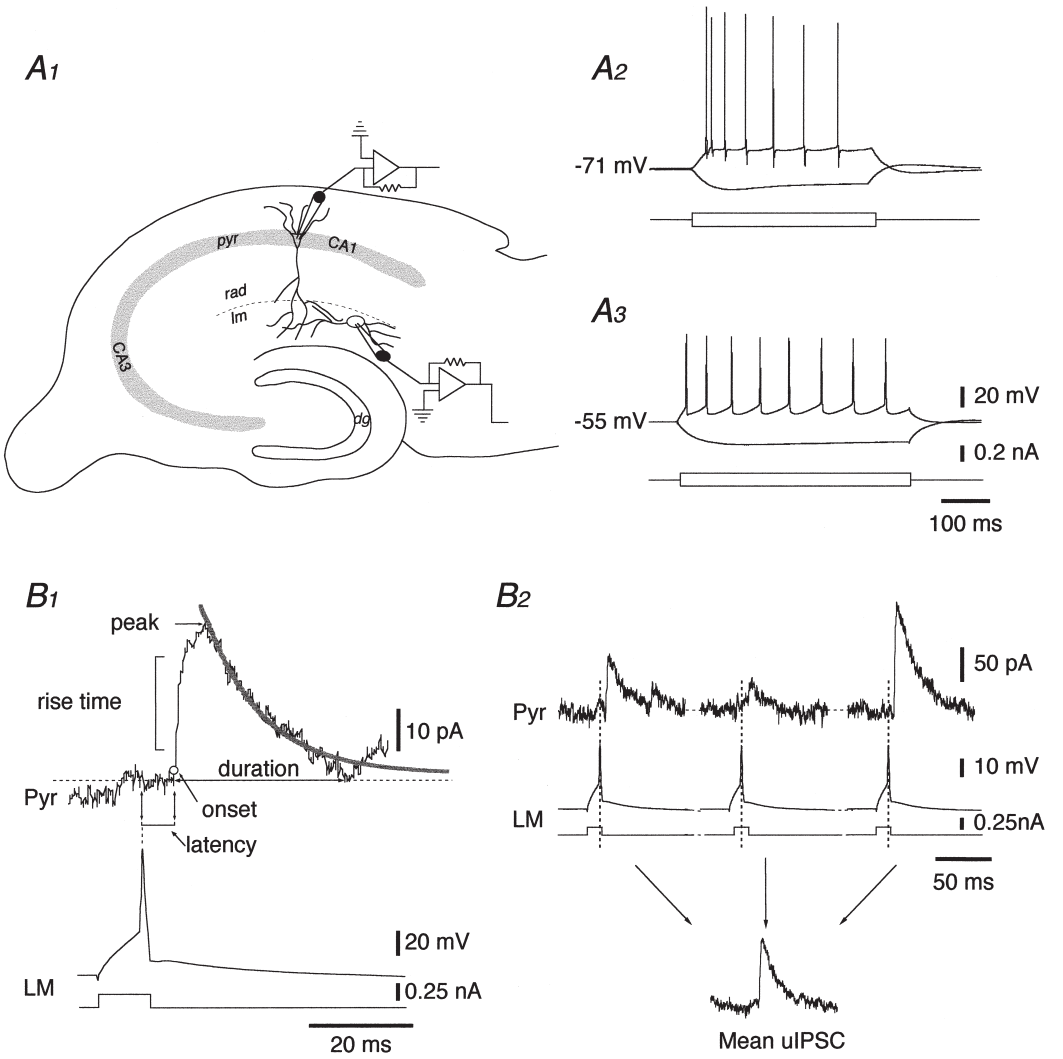


**Figure 1. Recordings and analysis of uIPSCs**

Diagram of the experimental arrangement (*A*1). *pyr*, stratum pyramidale; *rad*, stratum radiatum; *lm*, stratum lacunosum-moleculare; *dg*, dentate gyrus. A pyramidal cell (*A*2) and a LM interneurone (*A*3) were recorded in the whole-cell patch-clamp configuration. *B*1, definition of the parameters of uIPSC recorded in voltage-clamp mode from a pyramidal cell (Pyr) after an action potential induced by current injection in the LM interneurone (LM). *B*2, measurement of the mean uIPSC. Each uIPSC was sampled into 100 ms events, taking as reference the peak of the presynaptic action potential, and averaged.

experiments, followed by pair-wise comparisons using Bonferroni tests. The level of statistical significance was set at $P < 0.05$. Mean values are given ± S.E.M.

## RESULTS

Of 295 lacunosum-moleculare interneurone–pyramidal cell (LM–PYR) pairs obtained, 33 were found to be synaptically connected, which corresponds to 11.2% of synaptic connections. Obviously this percentage does not reflect the intrinsic connectivity in the intact hippocampus, since some axon collaterals and dendrites were probably severed in 300 $\mu$m thick slices, but gives an indication of the sparseness of these synaptic connections in our experimental conditions. Of the 33 synaptically connected LM–PYR pairs, 23 had stable and distinguishable uIPSCs and were included in the analysis.

### Morphological and electrophysiological characteristics of interneurones

To identify morphologically the interneurones recorded, cells were stained with fluorescent dyes ($n = 16$) or biocytin ($n = 6$). Morphological information was obtained for 11 LM interneurones with an intact soma. These interneurones had a morphology typical of stellate cells described previously (Ramon y Cajal, 1911; Lacaille & Schwartzkroin, 1988). An example of the typical morphology of a synaptically connected LM–PYR pair is illustrated in Fig. 2. The soma of LM interneurones (diameter 18.5 ± 1 $\mu$m, $n = 11$) was located in stratum lacunosum-moleculare or near its border with stratum radiatum and was fusiform in shape. The cell body of six interneurones was oriented parallel to stratum pyramidale, whereas in five others it was oriented vertically. The dendritic tree was typically bitufted and often varicose, with a predominantly horizontal orientation and arborisations into stratum lacunosum-moleculare and radiatum. Some branches often reached stratum pyramidale (e.g. Fig. 2). In the large majority of the recordings, the postsynaptic target domains of presynaptic interneurones were not determined. In two pairs, the axon was visualised and found to originate from the soma or a main proximal dendrite (Fig. 2). Axon

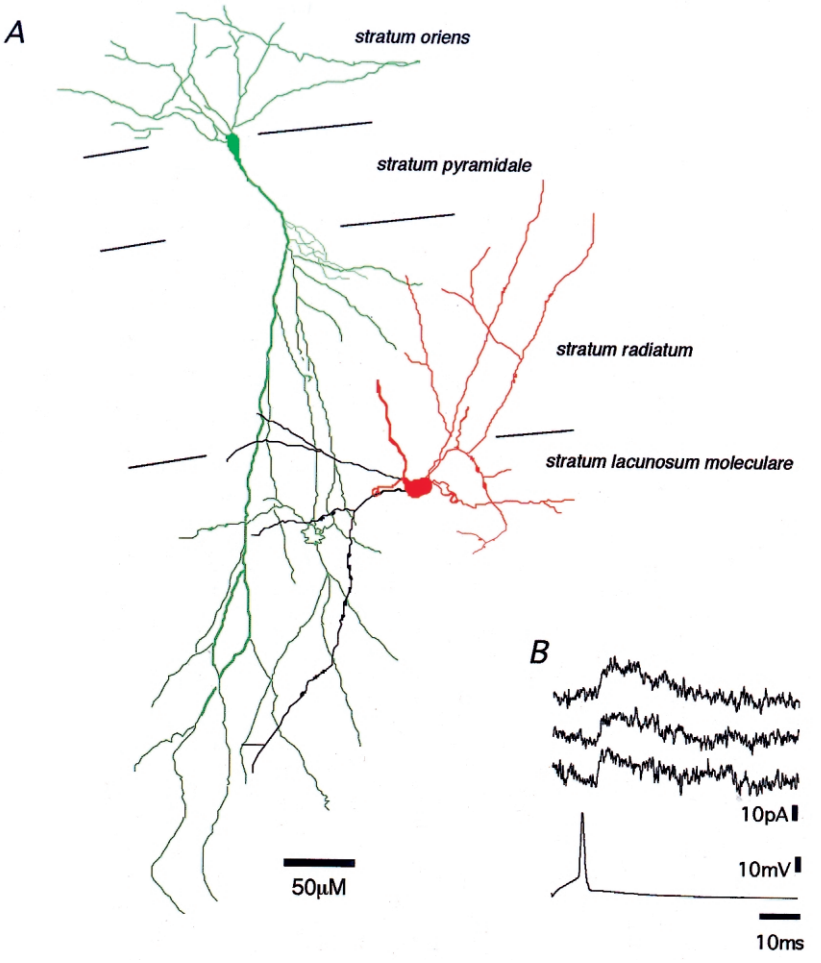


**Figure 2. Camera lucida drawing of a synaptically connected LM interneurone and pyramidal cell pair labelled with biocytin**

*A*, the soma and dendrites of the interneurone are shown in red, the axon in black. The pyramidal cell processes are shown in green. *B*, example of unitary synaptic currents recorded in this pyramidal cell following action potentials in the interneurone.

collaterals were parallel to the pyramidal cell layer and arborised predominantly in stratum radiatum and lacunosum-moleculare, as described previously (Lacaille & Schwartzkroin, 1988).

Interneurones had a mean resting membrane potential of $-65.4 \pm 1.4$ mV, with an input resistance of $258.1 \pm 17.3$ MΩ ($n = 23$). Depolarising current pulses generally elicited overshooting action potentials ($83.1 \pm 3.4$ mV) that had a duration of $2.7 \pm 0.1$ ms. As previously described (Lacaille & Schwartzkroin, 1988; Williams *et al.* 1994), these interneurones are characterised by a large spike afterhyperpolarisation, a small rectification during hyperpolarising current pulses, and a slight frequency accommodation during repetitive firing (Fig. 1*A*3). As previously reported (Lacaille & Schwartzkroin, 1988), some membrane properties of pyramidal cells were different from those of inter-

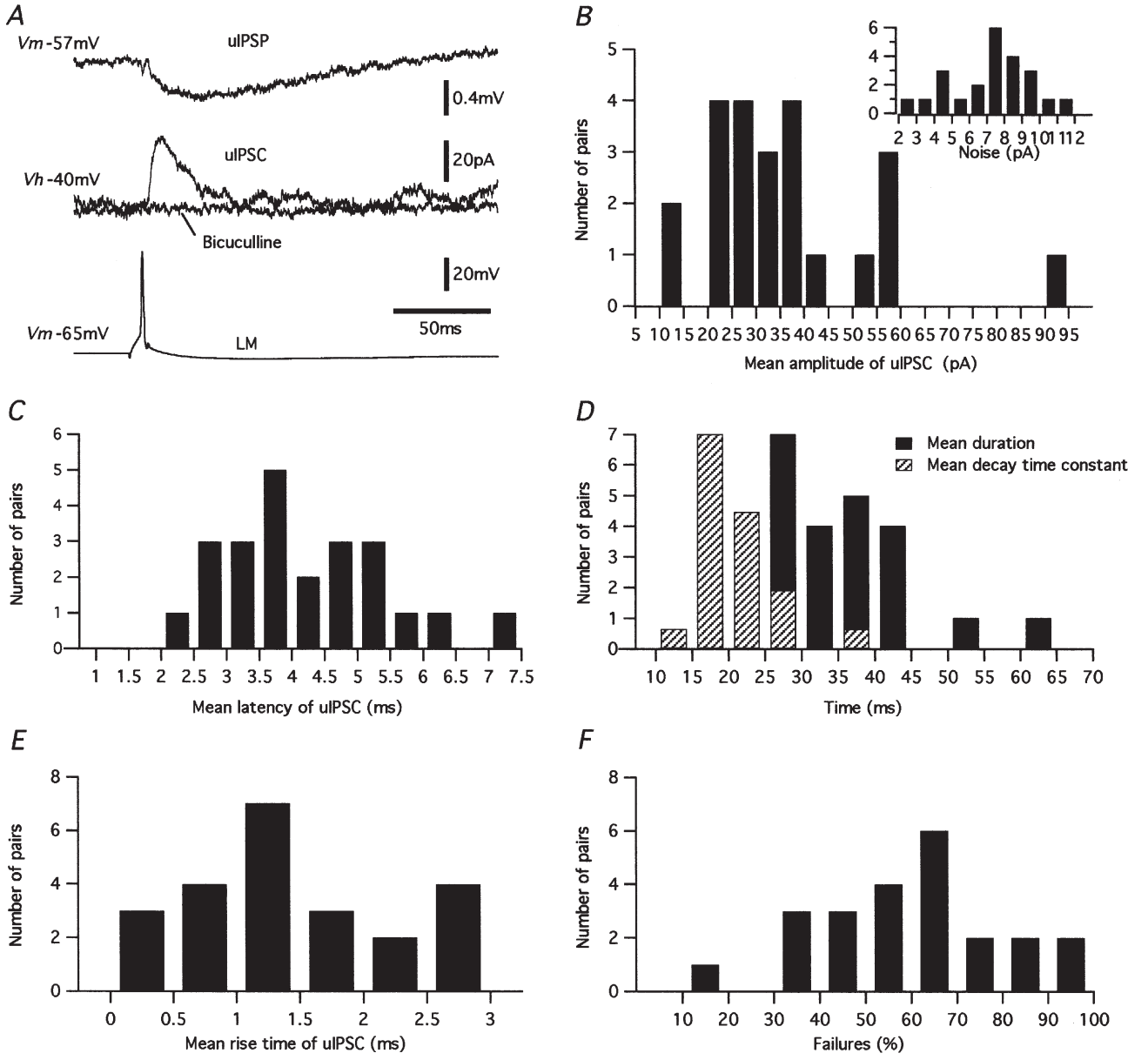


**Figure 3. Properties of $GABA_A$ uIPSCs between LM interneurones and pyramidal cells**

*A*, in a connected LM–PYR pair, an action potential in the presynaptic interneurone (LM, bottom trace) triggers a hyperpolarisation of the pyramidal cell (Pyr) in current-clamp mode at resting membrane potential ($V_m$, top trace) or an outward uIPSC in voltage-clamp mode with the membrane held at −40 mV ($V_h$, second trace). The uIPSC was completely antagonised by bicuculline (25 μM). *B*, distribution of mean uIPSC amplitude and background noise (inset) for all recorded pairs ($n = 23$). *C–F*, distribution of mean latency (*C*), duration and decay time constant (*D*), rise time (*E*) and failure rate (*F*) of uIPSCs for all pairs.

neurones: the average resting membrane potential was $-61.7 \pm 1.0$ mV, the input membrane resistance $185 \pm 15.6$ MΩ, the spike amplitude $130.9 \pm 3.0$ mV and the duration $2.9 \pm 0.08$ ms (compare *A*2 and *A*3 in Fig. 1). In the absence of glutamate blockers, action potentials in pyramidal cells never elicited inhibitory or excitatory synaptic currents in LM interneurones (Lacaille & Schwartzkroin, 1988).

### $GABA_A$ uIPSCs between LM interneurones and pyramidal cells

In synaptically connected pairs, single action potentials, induced by current pulses (0.1–0.6 nA, 5–20 ms), in LM interneurones, produced an uIPSP in pyramidal cells when recorded in current-clamp mode, or an outward uIPSC in voltage-clamp mode with the pyramidal cell held at −40 mV (Fig. 3*A*). Bath application of the $GABA_A$ antagonist bicuculline (25 μM) totally abolished these responses in all pairs tested ($n = 13$ pairs; Fig. 3*A*). No evidence was found of a $GABA_B$ component in these synaptic responses, indicating that uIPSCs triggered in pyramidal cells by single spikes in presynaptic LM interneurones involved solely $GABA_A$ receptors.

### Kinetics of $GABA_A$ uIPSCs

The histograms in Fig. 3 show the distribution of the mean uIPSC amplitude, latency, duration, decay time constant, rise time and failure rate for all synaptically connected pairs ($n = 23$; pyramidal cell, $V_h$ −40 mV). The mean amplitude and latency at these synaptic connections were $36.4 \pm 3.7$ pA (range 13.3–93.9 pA) and $4.2 \pm 0.2$ ms (range 2.4–7.2 ms), respectively. The mean rise time was $1.9 \pm 0.1$ ms (range 0.9–3.4 ms), the mean duration was $35.7 \pm 1.8$ ms (range 23.9–61.0 ms), and the mean decay time was $20.9 \pm 1$ ms (range 14.0–35.0 ms). The distribution of uIPSC amplitude was Gaussian ($P < 0.05$), and clearly distinct from background noise (inset, Fig. 3*B*) in each pair. The connections between LM interneurones and pyramidal cells exhibited a high failure rate ranging from 21.8 to 93.3 % (mean $59.2 \pm 4$ %). In five pairs tested in normal $Mg^{2+}$ and $Ca^{2+}$ concentrations (2 mM), the kinetics and failure rate of uIPSCs were not significantly different (data not shown).

In a given pair, postsynaptic responses evoked by a presynaptic action potential showed some variability (Fig. 4*A*1). First, presynaptic spikes sometimes failed to produce a postsynaptic current, or elicited uIPSCs which varied in amplitude (Fig. 4*A*1). In addition the latency of individual uIPSCs also showed some variability across successive trials (inset, Fig. 4*A*1). Given the variability of response, the amplitude, latency, rise time, duration and decay time constant were determined for each individual uIPSC in each synaptically coupled pair (see Methods). Correlation analysis indicated that uIPSCs kinetics were related to response amplitude, and this is illustrated for a typical LM–PYR pair in Fig. 4*A*. There was a significant linear negative correlation between uIPSC latency and amplitude ($P = 0.0176$, $r = -0.48$; latency range 5.6–4.1 ms; Fig. 4*A*2, ●). In addition, a significant positive correlation was found between uIPSC amplitude and rise time ($P = 0.0160$; $r = 0.49$; Fig. 4*A*2, ○), decay time constant ($P < 0.0001$; $r = 0.88$; Fig. 4*A*3, ◆) and duration ($P < 0.0001$; $r = 0.80$; Fig. 4*A*3, ◇). For these three latter parameters, the best fit was obtained with a monoexponential function ($y = a + b\exp(-cx)$; dotted lines in Fig. 4*A*2 and *A*3). These results indicate that uIPSC latency decreased linearly with increases in response amplitude, whereas uIPSC rise time, decay time constant and duration increased exponentially with increases in response amplitude. This characteristic behaviour was observed in all 23 pairs analysed. The data were then pooled and plotted as a function of the normalised uIPSC amplitude to obtain population estimates of the relationships (Fig. 4*B*1 and *B*2). The mean rise time, duration and decay time constant for the whole LM–PYR sample were, respectively, $2.6 \pm 0.7$ ms, $35.7 \pm 1.8$ ms and $20.6 \pm 1.2$ ms. As described for the response in a single pair, in the total population uIPSC latency decreased linearly ($P < 0.0001$; $r = -0.7987$) while the rise time, decay time constant and duration increased exponentially with uIPSC amplitude ($20.85 < r < 0.90$; Fig. 4*B*). The rise time and decay time constant were significantly correlated in the total sample ($P = 0.0004$; $r = 0.7767$).

### Voltage dependence of uIPSCs

Figure 5*A* shows the amplitude of the mean uIPSC at different postsynaptic membrane potentials for one synaptically coupled pair. When the amplitude of the mean uIPSC (including failures) was plotted as a function of holding membrane potential for all pairs tested (Fig. 5*B*), the current–voltage relation of uIPSC was non-linear and exhibited outward rectification as already described by Ouardouz & Lacaille (1997). The reversal potential of the response obtained from the current–voltage relation was −73.7 mV ($n = 6$ pairs; Fig. 4*B*). The calculated equilibrium potential for $Cl^-$ ions in our preparation using the Nernst equation was $E_{Cl} = -74.1$ mV, in good agreement with the observed reversal potential of $GABA_A$ uIPSCs. These results suggest that the unitary synaptic currents evoked in CA1 pyramidal cells by individual action potentials in LM interneurones are solely due to the opening of $Cl^-$ conductances under our experimental conditions. To determine if uIPSC kinetics were voltage dependent, the rise time, duration and decay time constant of the mean uIPSC, as well as its failure rate, were measured at different holding potentials (−40 to −90 mV). The rise time, duration and decay time constant were not significantly affected by the voltage, as shown in the graphs of Fig. 5*C* and *D*. In contrast, a significant increase

in the percentage of failures was observed at a holding potential of −70 mV. This apparent increase in failure rates is probably due to the membrane potential being close to the uIPSC reversal potential.

### Paired pulse stimulation

Paired pulse facilitation (PPF) and paired pulse depression (PPD) are frequency-dependent short-term changes at GABAergic synapses which have been suggested to depend on the presynaptic cell type activated (Gupta *et al.* 2000; Jiang *et al.* 2000; Maccaferri *et al.* 2000). In order to examine the behaviour of LM–PYR connections during paired pulse stimulation, two action potentials were elicited at 50 ms intervals with brief current pulses (0.25–0.6 nA; 5 ms) in LM interneurones and repeated at 0.2 Hz ($n = 6$ pairs; Fig. 6).

Bidirectional changes were observed during paired pulse stimulation across trials in individual cell pairs. In individual trials, the amplitude of the second uIPSC was

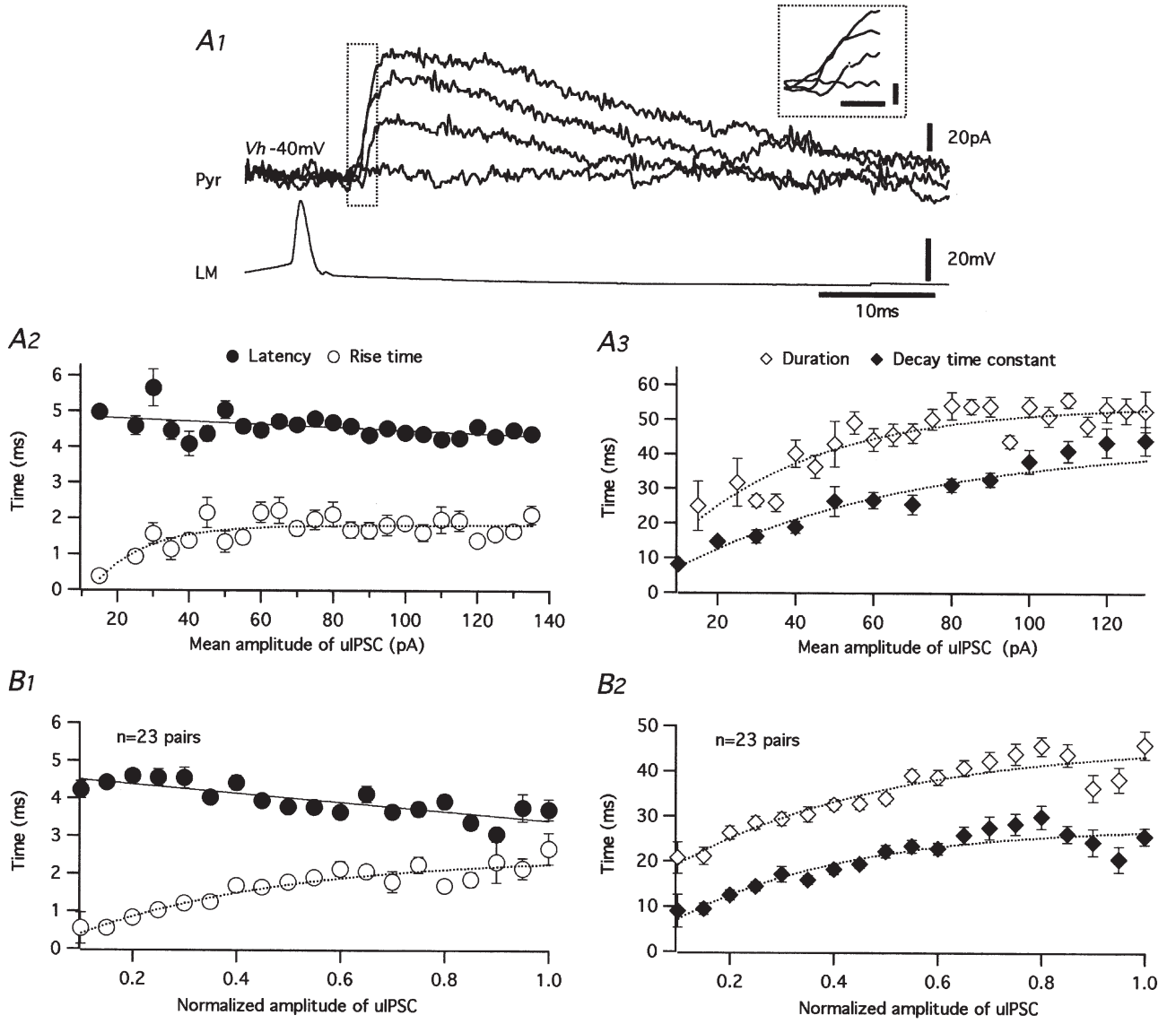


**Figure 4. Analysis of uIPSC kinetics**

*A*1, superposed unitary synaptic currents recorded from a pyramidal cell soma following single spikes in a LM interneurone ($V_m$ −65 mV). Inset, onset of uIPSCs at higher time resolution (horizontal bar 1 ms, vertical bar 20 pA). *A*2 and *A*3, plots of uIPSC latency, rise time (*A*2), duration and decay time constant (*A*3) as a function of amplitude for the same pair as in *A*1. *B*1 and *B*2, plots of mean uIPSC latency, rise time (*B*1), duration and decay time constant (*B*2) *versus* normalised uIPSC amplitude for the entire population of LM–PYR pairs. The continuous line illustrates the linear fit ($y = ax + b$) for latency and dotted lines indicate monoexponential fits ($y = a + b\exp(-cx)$) for the rise time, duration and decay time constant.

sometimes smaller (Fig. 6*A*1), similar (Fig. 6*A*2) or larger (Fig. 6*A*3) relative to the amplitude of the first uIPSC. This suggested that PPF or PPD could occur at individual LM–PYR connections. These results further implied that the probability of release for the second uIPSC may be influenced by the probability of release of the first uIPSC (Debanne *et al.* 1996; Ouardouz & Lacaille, 1997). Therefore, we performed two different analyses to study the effect of paired pulse stimulation on LM–PYR connections. We first examined the paired pulse ratio for individual trials ($uIPSC_2$/mean $uIPSC_1 \times 100$) as a function of the amplitude of first uIPSC (normalised to its maximal amplitude in each pair; Debanne *et al.* 1996). The graph of Fig. 6*B*1 (●) for all pairs tested ($n = 6$) shows the bidirectional behaviour that was a monoexponential function of the amplitude of the first uIPSC ($P < 0.05$; $r = -0.7$). At individual connections, a significant negative correlation ($r$ range: −0.83 to −0.41) was found in the three pairs for which the number of events permitted the analysis. The transition from facilitation to depression was estimated from the intersection between the exponential fit and the paired pulse ratio value of 100 %, giving a value of 26 % of the normalised uIPSC1 (arrow in Fig. 6*B*1). For the six pairs examined, the paired pulse ratios obtained when the first uIPSCs were smaller than this transition value and those obtained when the

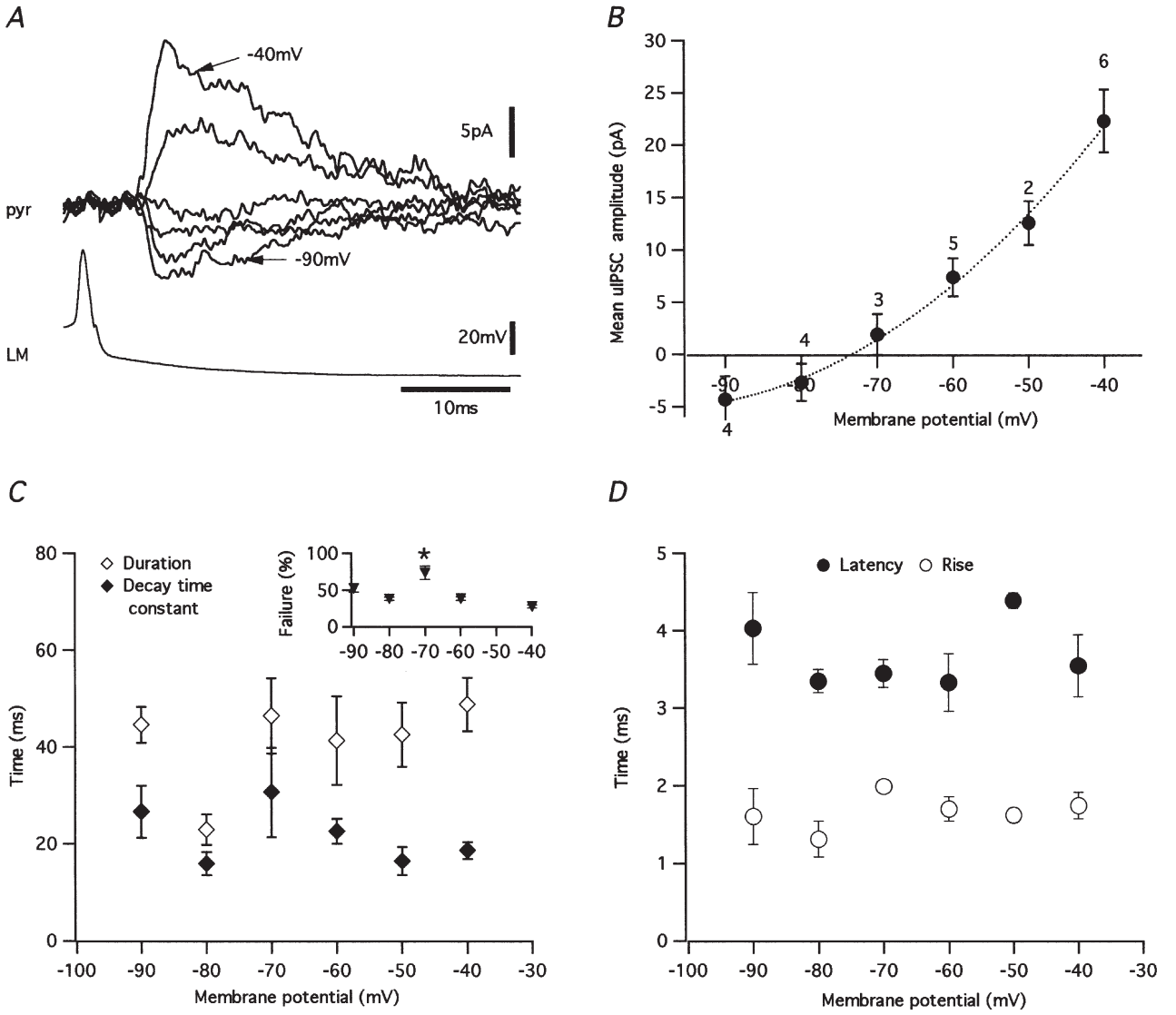


**Figure 5. Voltage sensitivity of uIPSCs**

*A*, superimposed mean uIPSCs recorded from a pyramidal cell at holding potentials between −40 and −90 mV (−10 mV increments). The reversal potential of the mean uIPSC in this cell was near −70 mV; (interneurone, $V_m$ −75 mV). *B*, plot of peak amplitude of mean uIPSCs *versus* holding potential for all pairs tested (number above each point indicates number of pairs). *C* and *D*, graphs of mean duration and decay time constant (*C*), failure rate (inset in *C*), rise time and latency (*D*) *versus* membrane potential for all connections tested. Only failure rate was significantly increased at a holding potential of −70 mV (* $P < 0.05$).

uIPSCs were larger than the transition value were significantly different (122.9 ± 7.0 % *vs.* 78.8 ± 1.7 %, respectively). The inset in Fig. 6*B*1 shows the same analysis for paired pulse ratios at a 5 s inter-stimulus interval for four pairs. The continuous line represents the linear fit from the plot ($r = 0.03$) and shows the lack of a significant effect at this long interval. At four individual connections, no significant correlation was observed ($r$ range: −0.05–0.2). In the two remaining pairs, a significant positive linear correlation was observed due to a high frequency of occurrence of large amplitude uIPSCs during this recording period (mean amplitudes were 56.3 ± 3.0 pA ($r = 0.35$) and 93.9 ± 2.0 pA ($r = 0.28$)). In a second step, we investigated the correlation between the amplitude of first and second uIPSCs at 50 ms inter-stimulus intervals (Kraushaar & Jonas, 2000). Figure 6*B*2 shows the plot of the amplitude of the second uIPSC as a function of the first uIPSC, both normalised to the mean amplitude of the first uIPSC in each pair ($n = 6$) (Kraushaar & Jonas, 2000). A significant linear negative correlation (continuous line in Fig. 6*B*2) was found between the first and second uIPSCs ($P < 0.05$, $r = -0.23$). At individual connections, a significant linear negative correlation was found in the three cases for which a sufficient number of events permitted such analysis. In contrast, when the amplitude of the second uIPSC was expressed as a function of the first uIPSC with uIPSCs separated by long intervals (5 s, $n = 4$ pairs), no correlation was found. In the other two connections, a significant positive linear correlation was observed due to the frequent occurrence of large amplitude uIPSCs (see above). These results indicate that during paired pulse stimulation at 50 ms intervals when the first uIPSC was small the second uIPSC tended to be larger and conversely when the first uIPSC was large the second uIPSC was smaller.

It is interesting to note that averaging all trials of paired pulse stimulation masked the bidirectional behaviour shown at these synapses. Indeed, the amplitude of all second uIPSCs was not significantly different from the mean amplitude of all first uIPSCs in each pair ($n = 6$; Fig. 6*C*). Thus averaging of multiple trials does not reflect paired pulse modulation accurately, as previously reported at excitatory synapses (Debanne *et al.* 1996).

We also examined whether the occurrence of the first uIPSC modified the kinetics of the second $GABA_A$ uIPSC. The histogram in Fig. 6*C* shows that there was no significant variation in the latency, rise time, decay time constant or duration between the averaged second uIPSC and the first. This suggested a uniform paired pulse regulation of all release sites involved.

Paired pulse depression of GABAergic synaptic responses has been suggested to involve presynaptic $GABA_B$ receptors (Deisz & Prince, 1989; Davies & Collingridge, 1990; Davies *et al.* 1993). In order to test the involvement of $GABA_B$ receptors in the paired pulse depression of uIPSCs, the effects of the $GABA_B$ receptor antagonist CGP 55845 (1 μM) were investigated. In the presence of this compound, the bidirectional changes observed during paired pulse stimulation were still present, as illustrated for the ensemble of pairs tested (Fig. 6*B*1, ○, $n = 4$). For the four pairs examined, when the first uIPSC was larger than the transition value, the mean paired pulse ratio was not significantly different in the presence of CGP 55845 (83.7 ± 3.5 %) than in control conditions (78.8 ± 1.7 %). Similar results were obtained for first uIPSCs smaller than the transition value. Under these conditions, the paired pulse ratio was 122.9 ± 7 % in control and 111.1 ± 0.7 % in the presence of CGP 55845. Similarly, when the second uIPSC amplitude was plotted as a function of the first uIPSC amplitude (Fig. 6*B*2), a significant negative linear correlation ($P < 0.05$, $r = -0.24$) was also observed in the presence of CGP 55845 (dotted line in Fig. 6*B*2). Thus, paired pulse depression was still seen in our conditions, even if presynaptic $GABA_B$ receptors were blocked.

Finally, the amplitude of the first uIPSC was also unchanged in the presence of CGP 55845 (amplitude of the averaged first uIPSC: control 16.7 ± 6.8 pA, in CGP 55845 14.9 ± 5.5 pA; $n = 7$; Fig. 6*D*).

Altogether these data suggest that, first, synaptic connections between LM–PYR pairs exhibit both paired pulse facilitation and depression, second, this paired pulse modulation depends critically on presynaptic transmitter release during the first response (see Discussion) and, third, tonic presynaptic $GABA_B$ inhibition is absent at LM–PYR connections in our experimental conditions.

### Requirement for recruiting slow $GABA_B$ IPSCs

Interneurones in LM have been proposed to generate, in part, $GABA_B$ inhibition of CA1 pyramidal cells (Williams & Lacaille, 1992; Nurse & Lacaille, 1997). However, uIPSCs triggered by individual action potentials in LM interneurones were totally blocked by the $GABA_A$ antagonist bicuculline, without unmasking a $GABA_B$ component (see Fig. 3*A*). Since it has been suggested that repetitive activation (4–10 action potentials) of a presynaptic interneurone was necessary to activate postsynaptic $GABA_B$ IPSCs (Thomson & Destexhe, 1999), we examined synaptic currents evoked by repetitive presynaptic activation during current injections of 100–120 ms duration. In synaptically coupled pairs, a burst of action potentials elicited summating uIPSCs in the pyramidal cell (Fig. 7*A*1) that were totally abolished by bicuculline. Increasing the number of presynaptic action potentials (up to 9; mean frequency 69.3 ± 4.8 Hz, range 50–80 Hz, $n = 6$) failed to evoke any slow $GABA_B$ currents (Fig. 7*A*2). Similar results were found in all LM–PYR pairs tested ($n = 6$). In one pair, neurotransmitter release was further increased by using the potassium channel blocker 4-aminopyridine (Jarolimek & Misgeld, 1993; Debanne *et al.* 1997). In 100 μM 4AP, the transmission failure rate markedly diminished. However,

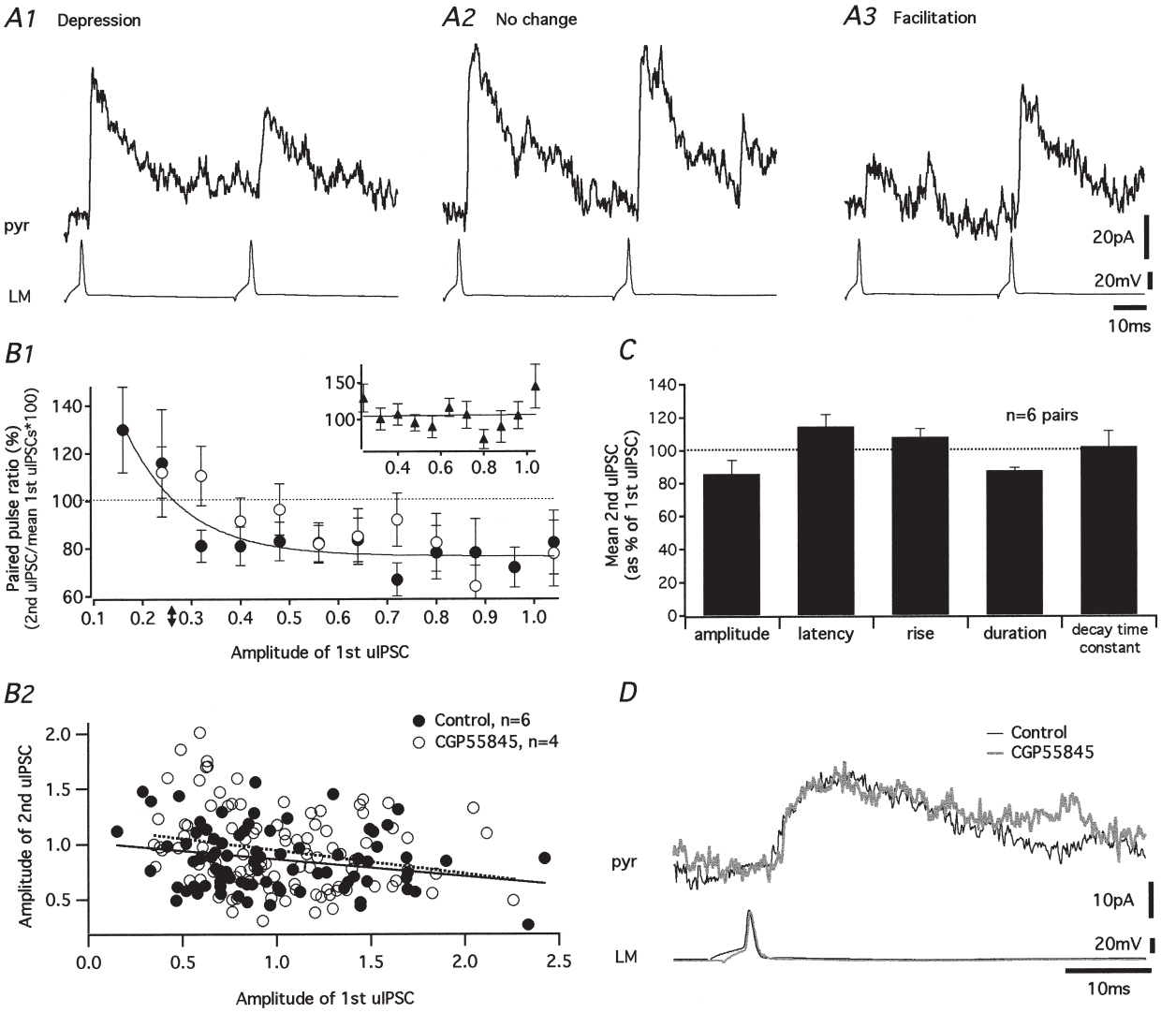


**Figure 6. Paired pulse modulation of uIPSCs**

*A*, paired stimulations were delivered at 50 ms interval to LM interneurones at 0.2 Hz. Three different trials are illustrated for the same LM–PYR pair showing depression (*A*1), no change (*A*2) or facilitation (*A*3) of the second uIPSC amplitude compared to the first. *B*, graph of the paired pulse ratio (second uIPSC/mean first uIPSCs × 100) as a function of the amplitude of the first uIPSC (normalised to the largest first uIPSC in each pair), for all pairs tested in control conditions (●) and in presence of CGP 55845 (○) (*B*1). Paired pulse depression (points under the dotted line) and paired pulse facilitation (points above the dotted line) can be clearly seen. In control conditions, the relationship was well fitted by an exponential equation $y = a + b\exp(-cx)$ where $a = -76.5$, $b = 210.2$ and $c = -8.3$ ($P < 0.05$; $r = -0.7$). Arrow on the $x$-axis indicates the transition point from facilitation to depression obtained from the exponential function. In control conditions this transition point was at 26 % of the maximal amplitude of the first uIPSC. The inset shows a similar analysis for paired pulse ratios at 5 s intervals and the continuous line represents the linear regression ($r = 0.03$, $n = 4$ pairs) obtained from the plot indicating an absence of paired pulse modulation at this interval. *B*2, plot of second uIPSC as a function of first uIPSC for all pairs tested in control conditions (●) and in presence of CGP55845 (1 $\mu$M; ○). Amplitude was normalised to the mean first uIPSC in each pair. The continuous line represents the linear regression ($P < 0.05$; $r = -0.23$) in control conditions and the dashed line the linear regression obtained in presence of CGP55845 ($P < 0.05$; $r = -0.24$). *C*, histogram of the amplitude, latency, rise time, duration and decay time constant of the averaged second uIPSC expressed as a percentage of the averaged first uIPSC. Parameters were not significantly changed during paired pulse stimulation. *D*, superimposed traces from a different pair from that shown in *A*, showing that the averaged first uIPSC triggered by single presynaptic action potentials (bottom traces) was similar in control conditions (black trace) and in the presence of CGP 55845 (grey trace).

repetitive activation of the presynaptic LM cell still failed to produce any detectable slow $GABA_B$ currents in the pyramidal neurone (data not shown).

Next, we examined the conditions necessary to evoke slow $GABA_B$ IPSCs using minimal extracellular stimulation. IPSCs were evoked in pyramidal cells using a bipolar theta glass electrode filled with ACSF and placed in stratum radiatum. In the presence of blockers of glutamatergic synaptic transmission (AP5 and CNQX), the intensity of stimulation was progressively adjusted to a threshold value ($T$) for a single pulse (23–250 $\mu$A,

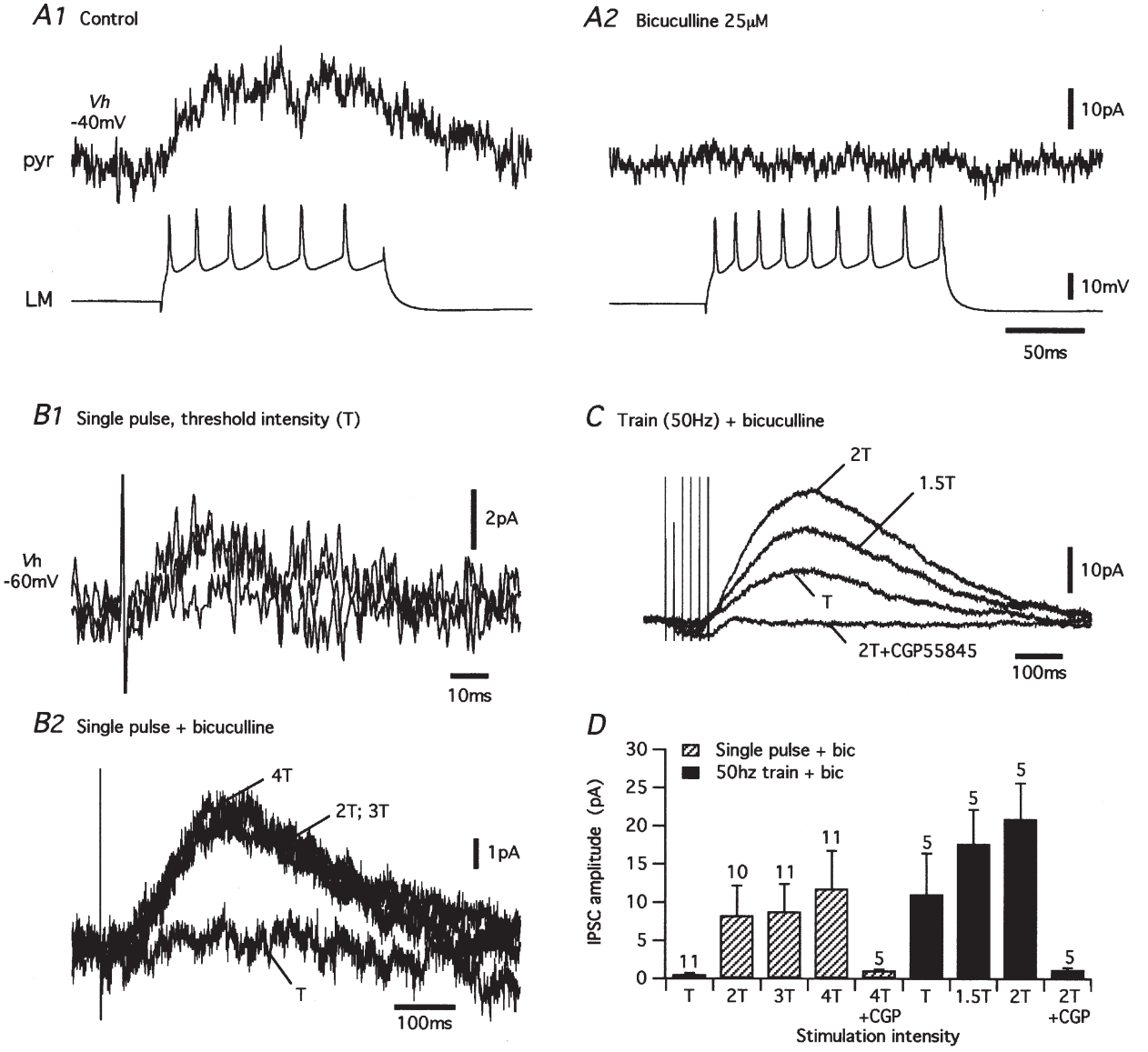


**Figure 7. Recruitment of $GABA_B$ slow IPSCs by extracellular stimulation**

*A*, repetitive activation of individual LM interneurones failed to activate $GABA_B$ currents. A burst of action potential potentials in a LM interneurone (−55 mV) evoked uIPSCs that summated in control conditions (*A*1) and were suppressed by addition of bicuculline. Increasing the number of presynaptic action potentials failed to recruit additional synaptic currents (*A*2). *B–D*, IPSCs evoked by extracellular stimulation. *B*, single pulse stimulations (0.5 ms, 0.2 Hz) at threshold intensity using a theta glass electrode in stratum radiatum evoked in pyramidal cells all-or-none fast IPSCs (*T*; *B*1). Three traces with two IPSCs and a failure are superimposed. These minimally evoked IPSCs were completely blocked by bicuculline (*B*2). However, increasing stimulation intensity to 2–4*T* recruited a slow IPSC (*B*2 and *D*). Note different time scales in *B*1 and *B*2. *C*, a short 50 Hz train of stimulation at *T* intensity in bicuculline recruited slow IPSCs. Increases in stimulation intensity (1.5–2*T*) increased the slow IPSC amplitude. *D*, histogram of mean IPSC amplitude with single pulse and 50 Hz train of stimulation at different intensities in the presence of bicuculline. Number above each bar indicates the number of cells tested in each condition. Slow IPSCs were completely blocked by the $GABA_B$ antagonist CGP 55845 (1 $\mu$M).

0.5 ms) that evoked all-or-none IPSCs (Fig. 7*B*1). Bicuculline was then applied, which completely blocked minimal IPSCs evoked by threshold single pulses in all cells tested ($n = 5$; Fig. 7*B*2 and *D*). Increasing the stimulation intensity (2*T*, 3*T*, 4*T*) of single pulses in the presence of bicuculline recruited slow IPSCs in all cells tested. These slow IPSCs evoked by single pulse stimulation appeared to reach a maximum with 2*T* stimulation (see Fig. 7*B*2 and *D*, hatched bars), suggesting that a maximum number of presynaptic inhibitory fibres were recruited at this intensity. Slow IPSCs were also recruited when a 50 Hz train was applied at *T* stimulation (Fig. 7*C*). With stimulus trains, increasing stimulation intensity from *T* to 1.5–2*T* tended to increase the amplitude of the slow IPSCs (Fig. 7*C* and *D*, black bars). These slow IPSCs were completely blocked by the $GABA_B$ antagonist CGP 55845 ($n = 5$ cells for single pulse stimulation and for train; Fig. 7*D*). These data demonstrate that the failure to observe $GABA_B$ IPSCs following repetitive activation of single LM interneurones was not due to recording conditions, since $GABA_B$ IPSCs could be recorded with extracellular stimulation in stratum radiatum. The need to increase the intensity of single pulse extracellular minimal stimulation or to use trains of stimulation to recruit $GABA_B$ IPSCs suggests that the synaptic activation of postsynaptic $GABA_B$ receptors on pyramidal cells may require the recruitment and coactivation of several presynaptic GABAergic fibres.

## DISCUSSION

In the present study, we provide new information about the properties of synaptic connections between individual LM interneurones and pyramidal neurones in the CA1 hippocampus of adult rats. Our results show that (1) uIPSCs produced in the distal dendrites of pyramidal cells are detectable at the soma and exhibit relatively large amplitude; (2) these uIPSCs are $GABA_A$ receptor mediated and due to an increase in $Cl^-$ conductance; (3) the kinetics of uIPSCs in all LM–PYR connections are a function of peak amplitude; (4) individual LM–PYR connections exhibit paired pulse facilitation or depression independent of $GABA_B$ receptor activation; and finally, (5) repetitive stimulation of an individual interneurone fails to activate postsynaptic $GABA_B$ currents, suggesting that coactivation of several GABAergic fibres may be needed for their activation.

### $GABA_A$ unitary IPSCs between LM interneurones and pyramidal neurones

The properties of uIPSCs showed a normal distribution across the different pairs. Interestingly, failure rates were high (on average 60 %), indicating that transmission was not always reliable at these connections. The kinetics of uIPSCs also displayed a homogeneous relation to response amplitude in all pairs. Amplitude was inversely related to uIPSC latency and positively correlated to rise time, duration and decay time constant. It is interesting that similar relationships were not found for compound spontaneous IPSCs in granule cells (Williams *et al.* 1998). Since these synapses appear located proximal to the granule cell soma, the properties we found may be characteristic of distal dendritic synapses. Alternatively, given that the experimental conditions we found necessary for recording $GABA_B$ synaptic currents were not optimal for voltage-clamp control of dendrites, the relationship between response amplitude and kinetics may have been due to an inadequate voltage clamp of larger synaptic events. Similar recordings with improved voltage-clamp conditions for $GABA_A$ currents (Maccaferri *et al.* 2000; Kraushaar & Jonas, 2000) will be necessary to address this issue. In addition, the homogeneity of uIPSC properties observed in our experiments is consistent with the similar morphology of the labelled LM interneurones, which was typical of stellate cells (Lacaille & Schwartzkroin, 1988; Williams *et al.* 1994; Morin *et al.* 1996). However, we did not distinguish among the possible different subtypes of stellate cells in LM (Vida *et al.* 1998). Nevertheless, our findings that the synaptic connections displayed relatively uniform properties suggest that they may represent a single functional class.

Recent studies suggest that unitary synaptic currents provided by different classes of interneurones may vary in terms of kinetics, short-term plasticity and GABA receptors (Ouardouz & Lacaille, 1997; Banks *et al.* 1998; Jiang *et al.* 2000; Maccaferri *et al.* 2000). Maccaferri and collaborators (2000) reported that the kinetics of uIPSCs generated by different types of oriens-alveus interneurones are dependent on the targeted domains of pyramidal cells. Interneurones innervating distal dendrites of pyramidal cells are found to generate uIPSCs with slower rise times (> 3 ms) and decay time constants than interneurones targeting pyramidal cell somas, probably due to electrotonic filtering. The kinetics of uIPSCs produced by LM interneurones are very similar to those of uIPSCs generated by oriens interneurones which target pyramidal cell dendrites in LM (O–LM cells, rise time 6.2 ± 0.6 ms, decay time 20.8 ± 1.7 ms; Maccaferri *et al.* 2000). Conceivably, this similarity indicates that LM interneurones and O–LM interneurones innervate similarly distant dendritic areas of pyramidal cells via similar mechanisms.

The kinetics of $GABA_A$ uIPSCs measured in the present paper were faster than those evoked by loose cell-attached stimulation of unidentified LM interneurones (Ouardouz & Lacaille, 1997). Three main reasons could account for these differences. First, the number of presynaptic spikes elicited with loose cell-attached stimulation was not monitored, and thus multiple IPSCs

could have been included in these measurements. Second, interneurones in LM with a fusiform cell body were selectively chosen in the present study, and thus other subtypes of LM interneurones, perhaps generating slower uIPSCs, could have been excluded from the present study. Finally, uIPSC decay was found to be voltage dependent between −40 and 20 mV (Ouardouz & Lacaille, 1997) and uIPSCs were characterised at more negative membrane potentials in the present study.

### Short-term plasticity during paired pulse stimulation

In this study, presynaptic stimulation with paired pulses at 50 ms intervals revealed facilitation or depression of uIPSCs in individual pairs. Paired pulse facilitation has been extensively described in hippocampal excitatory pathways (Andreasen & Hablitz, 1994; Debanne *et al.* 1996) but has been more rarely observed at inhibitory synapses (Fleidervish & Gutnick, 1995; Ouardouz & Lacaille, 1997; Jiang *et al.* 2000). In contrast, paired pulse depression is well established at inhibitory connections (Deisz & Prince, 1989; Davies *et al.* 1993; Jensen *et al.* 1999; Jiang *et al.* 2000; Maccaferri *et al.* 2000).

Paired pulse depression of inhibitory responses has been attributed to the activation of presynaptic $GABA_B$ autoreceptors (Davies *et al.* 1993) that reduce $Ca^{2+}$ influx in presynaptic terminals (Wu & Saggau, 1997) and, thus, decrease transmitter release. The paired pulse depression observed in LM–PYR pairs in the present study did not involve such $GABA_B$ receptor-mediated mechanisms since it was not affected by the $GABA_B$ receptor antagonist CGP 55845. $GABA_B$-independent paired pulse depression of unitary IPSCs has also been reported by Wilcox & Dichter (1994) in cultured hippocampal neurons (see also Jiang *et al.* 2000). At both excitatory and inhibitory synapses, the occurrence of paired pulse depression or facilitation has been suggested to be a function of baseline release probability (Katz & Miledi, 1968; Debanne *et al.* 1996; Jiang *et al.* 2000). Paired pulse facilitation may be due to residual $Ca^{2+}$ levels in presynaptic terminals following a first action potential that add to the $Ca^{2+}$ influx during the second action potential (Katz & Miledi, 1968; Jiang *et al.* 2000). Paired pulse depression, on the other hand, may be due to a transient decrease in quantal content resulting from depletion of the readily releasable vesicle pool during the first action potential (Stevens & Wang, 1995; Debanne *et al.* 1996; Jiang *et al.* 2000). Indeed in a recent study, Jiang and collaborators (2000) showed that the direction of paired pulse plasticity at unitary synapses between stratum radiatum interneurones and pyramidal cells varied with extracellular $Ca^{2+}$ concentration and release probability. In all pairs with high probability of failures that exhibited preferentially paired pulse facilitation, increasing the extracellular $Ca^{2+}$ concentration increased release probability and converted paired pulse facilitation to paired pulse depression. Similar presynaptic mechanisms may be responsible for paired pulse facilitation and depression at LM–PYR connections. If the first uIPSC is large, the readily releasable vesicle pool in the presynaptic terminals is diminished and is not restored in the 50 ms interval between spikes, leading to a second uIPSC of smaller amplitude. In such a scheme, the transition value from paired pulse facilitation to depression may correspond to the uIPSC amplitude at which the facilitation due to residual $Ca^{2+}$ levels is overcome by the depletion of the readily releasable vesicle pool. Our results indicate that in our conditions, this occurred at about 25 % of maximal uIPSC amplitude. Our paired pulse experiments were carried out in elevated $Mg^{2+}$ and $Ca^{2+}$ concentrations (4 mM). It seems unlikely that these conditions significantly affected the paired pulse plasticity, since in control experiments the probability of evoked release (failure rate) in LM–PYR pairs was not different in normal and elevated $Mg^{2+}$ and $Ca^{2+}$ concentrations.

The type of short-term plasticity found at inhibitory synapses in the hippocampus has been reported to be dependent on the interneurone subtype (Pearce *et al.* 1995; Jiang *et al.* 2000; Maccaferri *et al.* 2000). This has been interpreted as evidence for a high degree of specialisation of inhibition by different interneurone subtypes (Gupta *et al.* 2000; Maccaferri *et al.* 2000). Using an average of many paired pulse events, the LM–PYR connections in our study would have been characterised as lacking short-term modulation. Although such analysis has value in discriminating between specific types of connections (Maccaferri *et al.* 2000; Jiang *et al.* 2000), our results indicate that such interpretations should be made with caution. The detailed analysis of paired pulse ratio as a function of the amplitude of the first uIPSC indicated that each connection undergoes paired pulse facilitation or depression depending on the amplitude of the first response. Similar analysis should be performed with other subtypes of interneurones to define more clearly their short-term plasticity. It is interesting to note that at dentate gyrus basket cell–granule cell connections, a similar analysis indicated the presence of paired pulse depression of presynaptic origin but was independent of previous release (Kraushaar & Jonas, 2000). Thus, paired pulse modulation appears specific to interneurone cell types at inhibitory connections in the hippocampus.

### Lack of $GABA_B$ response between single lacunosum-moleculare interneurones and pyramidal cells

In the present study, postsynaptic $GABA_B$ IPSCs were undetectable in pyramidal cells following the activation of a single presynaptic LM interneurone. A role has been suggested for interneurones in LM in generating $GABA_B$ inhibition of pyramidal cells using local application of

glutamate (Williams & Lacaille, 1992). The absence of $GABA_B$ IPSCs in our paired recordings was not due to an immature $GABA_B$ system, since $GABA_B$ IPSCs have been found to appear in CA1 pyramidal cells 2 weeks after birth and to increase gradually until postnatal days 35–45 (Nurse & Lacaille, 1999) and slices from adult rat were used in our study. Our observations that increasing release of GABA from individual interneurones, by either bursting discharges or 4-aminopyridine, failed to evoke a $GABA_B$ response in postsynaptic CA1 pyramidal cells, suggest that transmitter release from an individual stellate cell is insufficient to activate these receptors. Further, our observations that minimal stimulation at threshold, presumably activating a single presynaptic fibre, failed to trigger a $GABA_B$ response in pyramidal cells, whereas stimulation with higher intensity or trains recruited slow $GABA_B$ IPSCs, suggest that postsynaptic $GABA_B$ receptors require the coactivation of several GABAergic fibres. Our findings are in agreement with recent evidence that simultaneous release from several interneurones is necessary for GABA spillover and activation of postsynaptic $GABA_B$ receptors (Scanziani, 2000), as well as with previous reports that considerable extracellular stimulation (Dutar & Nicoll, 1988) or enhanced synaptic GABA levels achieved by inhibiting uptake (Thompson & Gahwiler, 1992; Scanziani, 2000) are required to evoke $GABA_B$ IPSCs in pyramidal cells. Altogether these different studies and our data indicate that, under physiological conditions, the synchronous stimulation of several GABAergic afferents is needed to overcome GABA uptake and activate postsynaptic $GABA_B$ receptors in pyramidal cells.

Although Ouardouz & Lacaille (1997) found that loose cell-attached stimulation of different types of CA1 interneurones elicited only pure $GABA_A$ IPSCs, they observed a tonic presynaptic $GABA_B$ inhibition of $GABA_A$ uIPSCs in some LM–PYR connections. Such tonic presynaptic $GABA_B$ action was not observed in our LM–PYR pairs. This discrepancy could be due to different extracellular solutions used in the two studies. We used ACSF with low $K^+$ and high $Ca^{2+}$–high $Mg^{2+}$ concentrations to reduce cellular excitability and spontaneous synaptic activity in slices, and this may have reduced tonic $GABA_B$ inhibition.

### LM interneurones and hippocampal network activity

Hippocampal interneurones influence the activity of pyramidal cells via two main types of local circuit synaptic interactions. Some interneurones like basket, axo-axonic, horizontal and vertical cells receive recurrent excitatory inputs from pyramidal cells, and generate feedback inhibition (Knowles & Schwartzkroin, 1981; Lacaille *et al.* 1987; Buhl *et al.* 1994*a*,*b*; Maccaferri & McBain, 1995). In contrast, LM interneurones do not receive such excitatory collaterals and mediate only feedforward inhibition (Kunkel *et al.* 1988; Lacaille & Schwartzkroin, 1988). The present study provides evidence that although LM interneurones synaptically contact distal dendrites of pyramidal cells, uIPSCs with relatively large amplitudes are detected under voltage clamp at the cell body. Under current clamp, the propagation of these synaptic responses results in relatively large amplitude synaptic potentials at the soma, as previously reported (Lacaille & Schwartzkroin, 1988; Vida *et al.* 1998). The precise physiological role of LM interneurones in the hippocampal circuit remains unclear, but these interneurones have intrinsic conductances that generate membrane potential oscillations in the theta frequency range (Chapman & Lacaille, 1999). Activation of cholinergic/muscarinic receptors can induce these membrane potential oscillations (Chapman & Lacaille, 1999). Furthermore, the rhythmic activation of these interneurones can provide rhythmic dendritic inhibition of pyramidal cells and pace their firing at theta frequency (Chapman & Lacaille, 1999). LM interneurones via their dendritic inhibitory synapses may thus play an important synchronisation role in the hippocampal CA1 region. Our results indicate that at the single cell level, this synchronisation is via $GABA_A$ synaptic mechanisms. Interestingly, $GABA_B$ mechanisms could be recruited in addition when a number of these interneurones become synchronously activated (Scanziani, 2000). It remains to be determined how this dendritic inhibition interacts with local dendritic conductances in pyramidal cells (Magee *et al.* 1995; Tsubokawa & Ross, 1996) to generate the network activity.

Alger, B. E. & Nicoll, R. A. (1982). Pharmacological evidence for two kinds of GABA receptor on rat hippocampal pyramidal cells studied *in vitro*. *Journal of Physiology* **328**, 125–141.

Andreasen, M. & Hablitz, J. J. (1994). Paired pulse facilitation in the dentate gyrus: a patch-clamp study in rat hippocampus in vitro. *Journal of Neurophysiology* **72**, 326–336.

Banks, M. I., Li, T. B. & Pearce, R. A. (1998). The synaptic basis of $GABA_{A,slow}$. *Journal of Neuroscience* **4**, 1305–1317.

Buhl, E. H., Halasy, K. & Somogyi, P. (1994*a*). Diverse sources of hippocampal unitary inhibitory postsynaptic potentials and the number of synaptic release sites. *Nature* **368**, 823–828.

Buhl, E. H., Han, Z. S., Lorincki, Z., Steshka, V. V., Karnup, S. V. & Somogyi, P. (1994*b*). Physiological properties of anatomically identified axo-axonic cells in the rat hippocampus. *Journal of Neurophysiology* **71**, 1289–1307.

Buzsaki, G. & Chrobak, J. J. (1995). Temporal structure in spatially organized neuronal ensembles: a role for interneuronal networks. *Current Opinion in Neurobiology* **5**, 504–510.

Chapman, C. A. & Lacaille, J.-C. (1999). Cholinergic induction of theta-frequency oscillations in hippocampal inhibitory interneurons and pacing of pyramidal cell firing. *Journal of Neuroscience* **19**, 8637–8645.

Collingridge, G. (1987). Synaptic plasticity. The role of NMDA receptors in learning and memory. *Nature* **330**, 604–605.

Davies, C. H. & Collingridge, G. L. (1990). The physiological regulation of synaptic inhibition by $GABA_B$ autoreceptors in rat hippocampus. *Journal of Physiology* **472**, 245–265.

Davies, C. H., Davies, S. N. & Collingridge, G. L. (1993). Paired pulse depression of monosynaptic GABA-mediated inhibitory postsynaptic responses in rat hippocampus. *Journal of Physiology* **424**, 513–531.

Debanne, D., Guerineau, N., Gahwiler, B. H. & Thompson, S. M. (1996). Paired pulse facilitation and depression at unitary synapses in rat hippocampus: quantal fluctuation affect subsequent release. *Journal of Physiology* **491**, 163–176.

Debanne, D., Guerineau, N. C., Gahwiler, B. H. & Thompson, S. M. (1997). Action-potential propagation gated by an axonal $I_{(A)}$-like $K^+$ conductance in hippocampus. *Nature* **389**, 286–289.

Deisz, R. A. & Prince, D. A. (1989). Frequency-dependent depression of inhibition in guinea-pig neocortex *in vitro* by $GABA_B$ receptor feed-back on GABA release. *Journal of Physiology* **412**, 513–541.

Dolphin, A. C. (1995). The G. L. Brown Prize Lecture. Voltage-dependent calcium channels and their modulation by neurotransmitters and G-proteins. *Experimental Physiology* **80**, 1–36.

Dutar, P. & Nicoll, R. A. (1988). A physiological role for $GABA_B$ receptors in the central nervous system. *Nature* **332**, 156–158.

Fleidervish, I. A. & Gutnick, M. J. (1995). Paired pulse facilitation of IPSCs in slices of immature and mature mouse somatosensory neocortex. *Journal of Neurophysiology* **73**, 2591–2595.

Freund, T. F. & Buzsaki, G. (1996). Interneurons of the hippocampus. *Hippocampus* **6**, 347–470.

Gupta, A., Wang, Y. & Markram, H. (2000). Organizing principles for a diversity of GABAergic interneurons and synapses in the neocortex. *Science* **287**, 273–278.

Jarolimek, W. & Misgeld, U. (1993). 4-Aminopyridine-induced synaptic $GABA_B$ currents in granule cells of the guinea-pig hippocampus. *Pflügers Archiv* **425**, 491–498.

Jensen, K., Lambert, J. D. & Jensen, M. S. (1999). Activity-dependent depression of GABAergic IPSCs in cultured hippocampal neurons. *Journal of Neurophysiology* **82**, 42–49.

Jiang, L., Sun, S., Nedergaard, M. & Kang, J. (2000). Paired pulse modulation at individual GABAergic synapses in rat hippocampus. *Journal of Physiology* **523**, 425–439.

Katz, B. & Miledi, R. (1968). The role of calcium in neuromuscular facilitation. *Journal of Physiology* **195**, 481–492.

Knowles, W. D. & Schwartzkroin, P. A. (1981). Local circuit synaptic interactions in hippocampal brain slices. *Journal of Neuroscience* **1**, 318–322.

Kraushaar, U. & Jonas, P. (2000). Efficacy and stability of quantal GABA release at a hippocampal interneuron-principal neuron synapse. *Journal of Neuroscience* **20**, 5594–5607.

Kunkel, D. D., Lacaille, J.-C. & Schwartzkroin, P. A. (1988). Ultrastructure of stratum lacunosum-moleculare interneurons of hippocampal CA1 region. *Synapse* **2**, 382–394.

Lacaille, J.-C., Mueller, A. L., Kunkel, D. D. & Schwartzkroin, P. A. (1987). Local circuit interactions between oriens/alveus interneurons and CA1 pyramidal cells in hippocampal slices: electrophysiology and morphology. *Journal of Neuroscience* **7**, 1979–1993.

Lacaille, J.-C. & Schwartzkroin, P. A. (1988). Stratum lacunosum-moleculare interneurones of hippocampal CA1 region. II. Intrasomatic and intradendritic recordings of local circuit synaptic interactions. *Journal of Neuroscience* **8**, 1411–1424.

Maccaferri, G. & McBain, C. J. (1995). Passive propagation of LTD to stratum oriens-alveus inhibitory neurons modulates the temporoammonic input to the hippocampal CA1 region. *Neuron* **15**, 137–145.

Maccaferri, G., Roberts, J. D. B., Szucs, P., Cottingham, C. A. & Somogyi, P. (2000). Cell surface domain specific postsynaptic currents evoked by identified GABAergic neurones in rat hippocampus *in vitro*. *Journal of Physiology* **524**, 91–116.

Magee, J.-C., Christofi, G., Miyakawa, H., Christie, B., Lasser-Ross, N. & Johnston, D. (1995). Subthreshold synaptic activation of voltage-gated $Ca^{2+}$ channels mediates a localised $Ca^{2+}$ influx into the dendrites of hippocampal pyramidal neurons. *Journal of Neurophysiology* **74**, 1335–1342.

Morin, F., Beaulieu, C. & Lacaille, J.-C. (1996). Membrane properties and synaptic currents evoked in CA1 interneuron subtypes in rat hippocampal slices. *Journal of Neurophysiology* **76**, 1–16.

Nurse, S. & Lacaille, J.-C. (1997). Do $GABA_A$ and $GABA_B$ inhibitory postsynaptic responses originate from distinct interneurones in the hippocampus? *Canadian Journal of Physiology and Pharmacology* **75**, 520–525.

Nurse, S. & Lacaille, J.-C. (1999). Late maturation of $GABA_B$ synaptic transmission in area CA1 of the rat hippocampus. *Neuropharmacology* **38**, 1733–1742.

Ouardouz, M. & Lacaille, J.-C. (1997). Properties of unitary IPSCs in hippocampal pyramidal cells originating from different types of interneurons in young rats. *Journal of Neurophysiology* **77**, 1939–1949.

Pearce, R. A., Grunder, S. D. & Faucher, L. D. (1995). Different mechanisms for use-dependent depression of two $GABA_A$-mediated IPSCs in rat hippocampus. *Journal of Physiology* **484**, 425–435.

Perez, Y., Chapman, C. A., Woodhall, G. L., Robitaille, R. & Lacaille, J.-C. (1999). Differential induction of long-lasting potentiation of inhibitory postsynaptic potentials by theta patterned stimulation versus 100 Hz tetanization in hippocampal pyramidal cells in vitro. *Neuroscience* **90**, 747–757.

Prince, D. A. (1978). Neurophysiology of epilepsy. *Annual Review of Neuroscience* **1**, 395–415.

Ramon y Cajal, S. (1911). Histologie du système nerveux de l'homme et des vertébrés, tome II. Maloine, Paris.

Scanziani, M. (2000). GABA spillover activates postsynaptic $GABA_B$ receptors to control rhythmic hippocampal activity. *Neuron* **25**, 673–681.

Stevens, C. F. & Wang, Y. (1995). Facilitation and depression at single central synapses. *Neuron* **14**, 795–802.

Thompson, S. M. & Gahwiler, B. H. (1992). Effects of the GABA uptake inhibitor tiagabine on inhibitory synaptic potentials in rat hippocampal slice culture. *Journal of Neurophysiology* **67**, 1698–1701.

Thomson, A. M. & Destexhe, A. (1999). Dual intracellular recordings and computational models of slow inhibitory postsynaptic potentials in rat neocortical and hippocampal slices. *Neuroscience* **92**, 1193–1215.

Tsubokawa, H. & Ross, W. N. (1996). IPSPs modulate spike backpropagation and associated $[Ca^{2+}]_i$ changes in the dendrites of hippocampal CA1 pyramidal neurons. *Journal of Neurophysiology* **76**, 2896–2906.

Vida, I., Halasy, K., Szinyei, C., Somogyi, P. & Buhl, E. H. (1998). Unitary IPSPs evoked by interneurons at the stratum radiatum-stratum lacunosum-moleculare border in the CA1 area of the rat hippocampus *in vitro*. *Journal of Physiology* **506**, 755–773.

Wilcox, K. S. & Dichter, M. A. (1994). Paired pulse depression in cultured hippocampal neurons is due to presynaptic mechanism independent of $GABA_B$ autoreceptor activation. *Journal of Neuroscience* **14**, 1775–1788.

Williams, S. & Lacaille, J.-C. (1992). $GABA_B$ receptor-mediated inhibitory postsynaptic potentials evoked by electrical stimulation and by glutamate stimulation of interneurons in stratum lacunosum-moleculare in hippocampal CA1 pyramidal cells in vitro. *Synapse* **11**, 249–258.

Williams, S., Samulack, D. D., Beaulieu, C. & Lacaille, J.-C. (1994). Membrane properties and synaptic responses of interneurons located near the stratum lacunosum-moleculare/radiatum border of area CA1 in whole-cell recordings from rat hippocampal slices. *Journal of Neurophysiology* **71**, 2217–2235.

Williams, S. R., Buhl, E. H. & Mody, I. (1998) The dynamics of synchronized neurotransmitter release determined from compound spontaneous IPSCs in rat dentate granule neurones *in vitro*. *Journal of Physiology* **510**, 477–497.

Woodson, W., Nitecka, L. & Ben-Ari, Y. (1989). Organization of the GABAergic system in the rat hippocampal formation: a quantitative immunocytochemical study. *Journal of Comparative Neurology* **280**, 254–271.

Wu, L. G. & Saggau, P. (1997). Presynaptic inhibition of elicited neurotransmitter release. *Trends in Neuroscience* **20**, 204–212.

**Acknowledgements**

The authors thank Drs N Haddjeri and D. Le Ray for comments on previous versions of the manuscript, and Novartis for the gift of CGP 55845. This research was funded by a grant to J.-C.L. from the Canadian Institutes of Health Research (MT-10848). J.-C.L. is a National Scholar of the Fonds de la Recherche en Santé du Québec (FRSQ), a member of the Groupe de Recherche sur la Système Nerveux Central (GRSNC) from the Fonds pour la Formation de Chercheurs et l'Aide à la Recherche (FCAR), and a member of an Equipe de recherche from FCAR. S.B. was supported by a postdoctoral fellowship from the GRSNC-FCAR.

**Corresponding author**

J.-C. Lacaille: Centre de recherche en sciences neurologiques, Département de physiologie, Université de Montréal, CP 6128, succ. Centre Ville, Montréal, Québec, Canada H3C 3J7.

Email: lacailj@ere.umontreal.ca